ELSEVIER

Biochimica et Biophysica Acta 1319 (1997) 99–108

BIOCHIMICA ET BIOPHYSICA ACTA
BBA

# Substitutions at position 146 of cytochrome *b* affect drastically the properties of heme $b_L$ and the $Q_o$ site of *Rhodobacter capsulatus* cytochrome $bc_1$ complex

A. Sami Saribaş [a], Huangen Ding [b,1], P. Leslie Dutton [b], Fevzi Daldal [a,*]

[a] *Department of Biology, Plant Science Institute, University of Pennsylvania, Philadelphia, PA 19104, USA*
[b] *Department of Biochemistry and Biophysics, Johnson Research Foundation, University of Pennsylvania, Philadelphia, PA 19104, USA*

Received 30 May 1996; revised 7 August 1996; accepted 11 September 1996

**Abstract**

The cytochrome (cyt) *b* subunit of ubihydroquinone: cytochrome *c* oxidoreductase ($bc_1$ complex) contains four invariant glycine (G) residues proposed to be essential for proper packing of the high and low potential ($b_H$ and $b_L$) hemes of the $bc_1$ complex. One of these residues, G146 located in the transmembrane helix C of cyt *b* of *Rhodobacter capsulatus*, was substituted with A and V using site-directed mutagenesis, and the effects of these substitutions on the properties of the ubiquinone oxidation ($Q_o$) site and heme $b_L$ of the $bc_1$ complex were analyzed. The mutants G146A and V produced properly assembled but catalytically defective $bc_1$ complexes that are unable to support photosynthetic growth. The steady-state ubihydroquinone: cytochrome *c* reductase activities of the mutant complexes were about one-tenth of that of a parental strain overproducing the wild-type enzyme. Similarly, their light-activated single turnover rates were significantly lower than those of a wild-type complex. The dark potentiometric titrations revealed no significant changes in the redox midpoint potentials ($E_{m,7}$) of the high ($b_H$) and low ($b_L$) potential hemes of cyt *b* in both G146A and V mutants. However, EPR spectroscopy of the [2Fe-2S] cluster of the $bc_1$ complex indicated that the $Q_o$ site of the mutant enzymes were unoccupied. Moreover, the $g_z$ signal of heme $b_L$, but not that of heme $b_H$, was modified both in G146A and V, suggesting that the geometry of its ligands has been distorted. These findings indicate that this region of cyt *b* must be well packed around heme $b_L$ since even a slight increase in the size of the amino acid side chain at position 146 (such as G to A) greatly perturbs the spatial conformation of heme $b_L$, alters substrate accessibility and binding to the $Q_o$ site, and renders the $bc_1$ complex inactive.

*Keywords:* Photosynthesis; Respiration; Electron transfer; Mutant; Cytochrome *b*; Ubihydroquinone oxidation site

Abbreviations: Bchl, bacteriochlorophyll; cyt, cytochrome; $bc_1$ complex, ubihydroquinone cytochrome *c* oxidoreductase; $b_L$, low potential heme; $b_H$, high potential heme; $E_h$, ambient potential; $E_{m,7}$, redox midpoint potential at pH 7.0; EPR, electron paramagnetic resonance; $Q_o$, ubihydroquinone oxidation site; $Q_i$, ubiquinone reduction site; $QH_2$, ubihydroquinone; Q, ubiquinone; [2Fe-2S], iron sulfur cluster of the Rieske FeS protein; DBH, 2,3-dimethoxy-5-decyl-6-methyl-1,4-benzohydroquinone; MOPS, (*N*-morpholino) propanesulfonic acid; PMS, *N*-methyldibenzopyrazine methosulfate; PES, *N*-ethyldibenzopyrazine ethosulfate; DAD, 2,3,5,6-tetramethyl-*p*-phenylenediamine (diaminodurene); TMPD, N,N,N′,N′ tetramethyl-*p*-phenylenediamine; 1,2 NQ 4S, 1,2 naphthoquinone-4-sulfonic acid; SHE, standard hydrogen electrode; Ps, photosynthesis; Res, respiration.

* Corresponding author. Fax: +1 (215) 898 8780; E-mail: fdaldal@sas.upenn.edu
[1] Present address: Department of Molecular and Cellular Toxicology, Harvard School of Public Health, Boston MA 02115, USA.


*PII* S0005-2728(96)00120-X

## 1. Introduction

The ubihydroquinone: cytochrome (cyt) *c* oxidoreductase ($bc_1$ complex) is a multisubunit integral membrane protein that catalyzes photosynthetic and respiratory electron transfer and vectorial proton translocation, thereby creating a proton motive force used for ATP production. This enzyme complex is found in many organisms extending from bacteria to eukaryotes, as well as in plants (in its $b_6f$ form) [1–4]. The bacterial complex is composed minimally of three subunits carrying four redox centers: cyt *b* protein with two non-covalently bound hemes $b_H$ ($E_{m,7} = 50$ mV) and $b_L$ ($E_{m,7} = -90$ mV) named after their high and low redox midpoint potentials, respectively; cyt $c_1$ with a covalently bound heme, and the FeS protein with a [2Fe-2S] center of Rieske type, which can be readily monitored by EPR spectroscopy in its reduced form. Cyt *b* protein is composed of eight (A to H) transmembranes, and at least one transversal, helices and provides the axial histidine ligands of the two heme groups (H97/H111 and H198/H212 located on the helices B and D, respectively) [5] (Fig. 1). Earlier experiments have established that heme $b_L$ is located on the positive side of the membrane, near the $Q_o$ site where oxidation of ubihydroquinone ($QH_2$) to ubiquinone (Q) takes place. On the other hand, heme $b_H$ is located near the

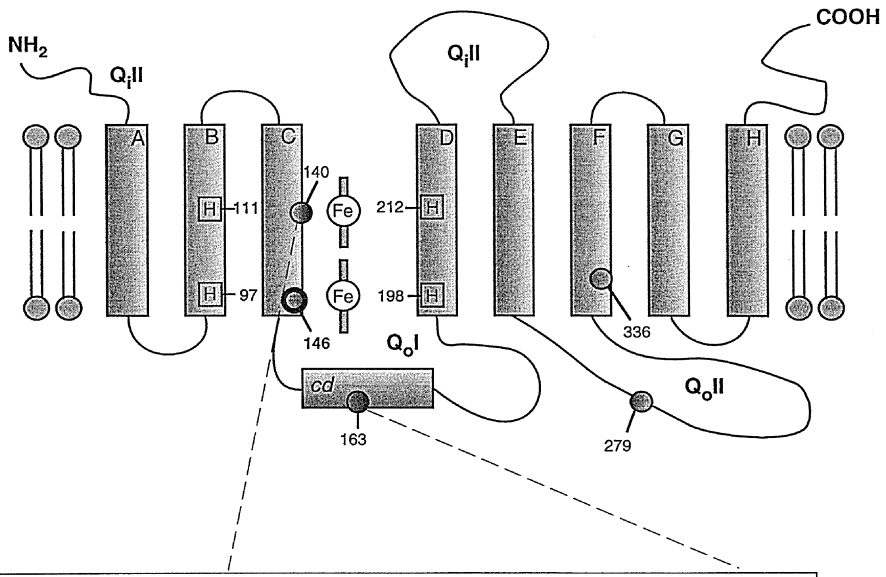


| | 140 | 146 | 163 |
|---|---|---|---|
| **Bacteria** | | | |
| *R. capsulatus* | M G T A F M G | Y V L P W G Q M S F W G A T V I T | |
| *R. rubrum* | M G T A F M G | Y V L P W G Q M S F W G A T V I T | |
| **Mitochondria** | | | |
| *S. cerevisiae* | I A T A F L G | Y C C V Y G Q M S H W G A T V I T | |
| *H. sapiens* | M A T A F W G | Y V L P W G Q M S F W G A T V I T | |
| *M. musculus* | M A T A F W G | Y V L P W G Q M S F W G A T V I T | |
| *L. smithii* | M A T A F V G | T M L P - - - - - - - - - - - - - | |
| *P. aurelle* | Q V V A F F G | L V L C C T H L E S I T L T I A A | |
| **Chloroplast($b_6$)** | | | |
| *S. oleracea* | A S F G V T G | Y S L P W D Q I G Y W A V K I V T | |
| *C. protothecoides* | V S F G V T G | Y S L P W D Q I G Y W A V K I V T | |
| *Nostoc* | V S F G V T G | Y S L P W D Q V G Y W A V K I V S | |

Fig. 1. A topological model of *R. capsulatus* cyt *b* and sequence alignment of a region encompassing its amino acid 146 from various species. The G146 residue studied in this work is indicated by a black circle, and typed in bold face, and the sequence alignments shown was taken from Degli-Esposti et al. [28].

negative face of the membrane and is closer to the $Q_i$ site where ubiquinone is reduced to ubihydroquinone [6]. In *Rhodobacter capsulatus* $bc_1$ complex, the $Q_o$ site of cyt *b* has previously been defined using spontaneous mutations conferring resistance to various $Q_o$ site inhibitors [1,4]. According to these studies, it is formed by the $Q_o$I region encompassing the residues M140 to T163, and the $Q_o$II region extending from residues 279 to 336 (Fig. 1). Site-directed mutagenesis of several amino acid residues of interest in this region of cyt *b* has been carried out, and biochemical and biophysical characterizations of these mutants have yielded important information in respect to $Q_o$ site structure and catalysis [7–12]. For example, F144 [7,9–12] and G158 [7–9] are critical for $Q/QH_2$ accessibility and binding to the $Q_o$ site, and Y147 is essential for efficient $Q_o$ site oxidation [13] while T163 is required for proper subunit-subunit interactions in forming the $Q_o$ site of the $bc_1$ complex (Saribaş et al., in preparation).

The three-dimensional structure for the $bc_1$ complex is not yet complete [27], thus structural details encompassing the heme groups of cyt *b* are unknown. Tron et al. [14] have suggested that four invariant glycine (G) residues in yeast cyt *b*, the 13 residues spaced G33 (48, *R. capsulatus* numbering) and G47 (62) in helix A and G117 (132) and G131 (146) in helix C, are important for proper packing of the heme groups. It has been observed that in *Rhodobacter sphaeroides* G48 (also 48 in *R. capsulatus*) D mutation abolished assembly of the $bc_1$ complex, whereas G48V substitution affected the properties of heme $b_H$ and impaired the $Q_i$ site functions [15]. In addition, the spontaneous G131 (G146 in *R capsulatus*) S mutation encountered in yeast affected severely the assembly and stability of the $bc_1$ complex [16], revealing that this position plays a critical role for the structure of cyt *b*. However, the absence of a properly assembled $bc_1$ complex has precluded detailed analysis of the impacts of this mutation. In particular, the role of this remarkably well conserved G residue on the properties of heme $b_L$ and the $Q_o$ site remained unknown. Thus, using *R. capsulatus* genetic system, position 146 was substituted by site-directed mutagenesis with a small (A) and a larger (V) size amino acid residue. Here we report that these substitutions yield properly assembled but inactive $bc_1$ complexes with perturbed $Q_o$ site occupancy. Further, they cause drastic changes in the EPR line shape attributed to heme $b_L$, indicating that the size of the amino acid side chain residing at position 146 is critical for both the conformation of heme $b_L$ and the $Q/QH_2$ occupancy of the $Q_o$ site of the $bc_1$ complex.

## 2. Materials and methods

### 2.1. Culture, media and genetic methods

All *Escherichia coli* strains were grown in LB medium, and *R. capsulatus* strains in enriched MPYE or minimal Medium A, supplemented with an appropriate amount of desired antibiotics as described previously [17]. For *R. capsulatus* strains photoheterotrophic growth was in anaerobic jars using BBL GasPaks (Becton Dickenson). Routine recombinant DNA techniques were as described earlier [18]. Site-directed mutations G146A and V were constructed using phage M13-73R2BC1 as a template, and the degenerate oligonucleotide 5′-CAGCACGTAG**A**/**G**CCATGAAGG-3′ as a primer [13]. Briefly, following mutagenesis and screening by DNA sequence analysis, a 500 basepair *Eco*RI-*Sma*I fragment containing the desired mutation was excised from the replicative form of the corresponding mutant phage, and exchanged with its wild-type counterpart on plasmid pMTS1 that carries a wild-type copy of *fbcFBC(petABC)* operon encoding the $bc_1$ complex. The plasmids pBG146A and pBG146V thus obtained were conjugated by triparental crosses into *R. capsulatus* strain MT-RBC1 carrying a deletion covering the entire *fbc(pet)* operon. These mutations were reconfirmed by sequencing of the plasmid DNA extracted from the transconjugants.

### 2.2. Biochemical and biophysical methods

Chromatophore membranes were prepared in 50 mM MOPS buffer (pH 7.0) containing 100 mM KCl, 1 mM EDTA and 1 mM PMSF using a French Pressure cell as described previously [13]. Bacteriochlorophyll (Bchl) concentration was measured spectroscopically using an $\epsilon_{775}$ of 75 $mM^{-1}$ $cm^{-1}$, and the amount of protein was determined according to

Lowry et al. [19] after extraction of pigments using a mixture of chloroform:acetone in 7:2 ratio.

Optical potentiometric titrations from 300 to −200 mV to determine the $E_{m,7}$ of the hemes $b_L$ and $b_H$ were performed according to Dutton [20], using a double beam spectrophotometer (Biomedical Instrumentation Group, University of Pennsylvania). An amount of chromatophores containing 50 μM Bchl were used in the presence of 25 μM 1,4 benzoquinone, 25 μM 1,2 naphthoquinone, 20 μM *N*-methyldibenzopyrazine methosulfate (PMS), 20 μM *N*-ethyl dibenzopyrazine ethosulfate (PES), 50 μM 2,3,5,6-tetramethyl-*p*-phenylenediamine (diaminodurene, DAD), 25 μM 2-hydroxy-1,4-naphthoquinone, 20 μM pyocyanine and 25 μM 1,4-naphthoquinone as mediators. Similarly, flash-activated (8 μs actinic light pulse), time-resolved cyt $b_H$ and cyt *c* re-reduction single turnover kinetics were performed as before [21] using a dual-wavelength spectrophotometer (Biomedical Instrumentation Group, University of Pennsylvania). For these experiments an amount of chromatophores containing 0.20 μM bacterial reaction center was used in the presence of 3 μM valinomycin, 2.5 μM PMS, 2.5 μM PES, 6 μM DAD, 10 μM 2-hydroxy-1,4-naphthoquinone, and 10 μM $FeCl_3$-EDTA. Reaction center concentration was determined by measuring the optical absorption difference between 605 and 540 nm after four flashes at $E_h = 370$ mV and using an extinction coefficient of 29.8 $mM^{-1}$ $cm^{-1}$. Samples were poised at desired redox potentials ($E_h$) using sodium dithionite or potassium ferricyanide, and antimycin (10 μM) or myxothiazol (5 μM) was added as needed. Cyt *b* reduction and cyt *c* re-reduction were monitored at 560 *minus* 570 nm and 550 *minus* 540 nm, respectively, and the single turnover rates were calculated as in Gray et al. [21].

EPR spectroscopy was used to monitor the $Q/QH_2$ occupancy of the $Q_o$ site at different $E_h$ values (400 to −300 mV) via their known interactions with the [2Fe-2S] cluster of the FeS protein as described in detail by Ding et al. [7,10,11]. For these measurements, chromatophores were supplemented with 40 μM DAD, PMS, PES, 2-hydroxy-1,4-naphthoquinone, phenazine, 1,4 naphthoquinone and $FeCl_3$-EDTA when the [2Fe-2S] cluster was monitored and 20 μM stigmatellin was added as needed. For the redox titrations of the [2Fe-2S] cluster, chromatophores were supplemented with 25 μM TMPD, DAD, 1,2 NQ 4S and 40 μM stigmatellin (in DMSO) was used. For the hemes $b_L$ and $b_H$ spectra, highly concentrated chromatophore preparations (approximately 1.2 mM BChl) were reduced with ascorbate. This poised the ambient potential $E_h$ at a value where the heme group of cyt $c_1$ is reduced while the hemes $b_L$ and $b_H$ are oxidized, thus remain paramagnetic and can be observed by EPR spectroscopy [22]. The spectra were taken using a Bruker EPR spectrometer model ESP-300E, equipped with a helium cryostat, under the following experimental conditions: (a) [2Fe-2S] cluster: temperature, 20 K; microwave power, 2 mW; modulation amplitude, 12.5 gauss; modulation frequency, 100 kHz; microwave frequency, 9.45 GHz; time constant, 40.9 ms; scan rate, 23.8 gauss/s; (b) hemes $b_L$ and $b_H$: temperature, 5 K; microwave power, 20 mW; modulation

Table 1
Phenotypic properties of *R. capsulatus* cyt *b* G146A and G146V mutants and biochemical properties of their $bc_1$ complexes

| Strains | Phenotype | DBH Activity [a] (%) | $Q_o \rightarrow b_H$ [b] $s^{-1}$ | Cyt *c* [b] $s^{-1}$ |
|---|---|---|---|---|
| pMTS1 (wt) | $Ps^+$ | 100 (100) [c] | 553 | 338 |
| MT-RBC1 ($bc_1^-$) | $Ps^-$ | 0.6 | – | – |
| pBG146A | $Ps^-$ | 11 (15) | 15 | 21 |
| pBG146V | $Ps^-$ | 10 (15) | 16 | 16 |

[a] DBH activity of a wild-type strain was determined to be 4376 nmol of cyt *c* reduced per min per mg of membrane protein in this instance, and normalized to 100%.
[b] $Q_o \rightarrow b_H$ and cyt *c* corresponds to electron transfer rates from $Q_o$ to $b_H$ and $Q_o$ to cyt *c*, respectively monitored at an $E_h$ of 100 mV.
[c] DBH activity presented in parentheses corresponds to the turnover number of the $bc_1$ complex in each strain. For this, the amount of the $bc_1$ complex in chromatophore membranes was estimated by measuring the total amount of cyt *b* (using reduced *minus* oxidized spectra and an absorption coefficient $\epsilon_{(560\text{-}574)} = 28$ $mM^{-1}$ [29]) in various strains. From this value that was found in a $bc_1^-$ mutant was subtracted. For a wild-type strain the turnover number of the $bc_1$ complex was in this instance 42.8 $s^{-1}$ and taken as 100%.

amplitude, 12.6 gauss, modulation frequency 100 kHz; microwave frequency, 9.45 GHz, time constant, 40.9 ms; scan rate, 9.53 gauss/s.

### 2.3. Chemicals

PMS, PES, TMPD and antimycin A were purchased from Sigma (St. Louis, MO). Myxothiazol and restriction enzymes were obtained from Boehringer-Mannheim Biochemicals. 2,3,5,6-tetramethyl-*p*-phenylenediamine (diaminodurene), 2-hydroxy-1,4-naphthoquinone were purchased from Aldrich. Stigmatellin was obtained from Fluka. Pyocyanine was a gift from Dr. D.E. Robertson (University of Pennsylvania). All other chemicals were reagent grade and purchased from commercial sources.

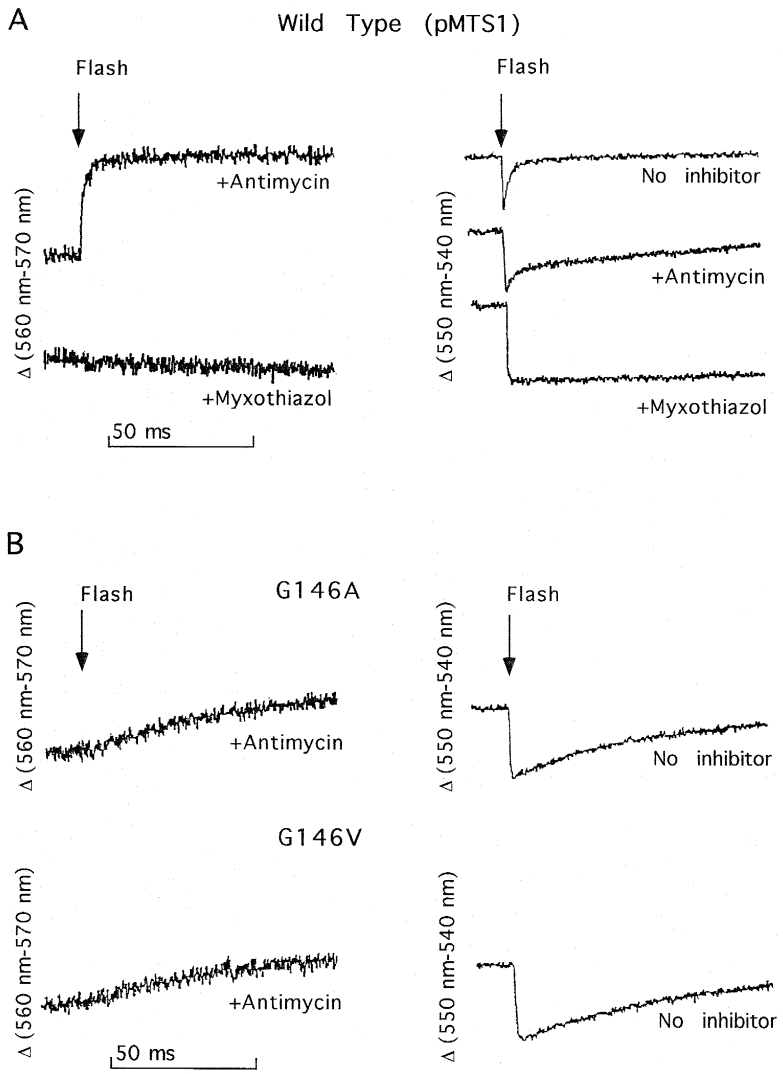


Fig. 2. Light-activated single turnover kinetics of cyt $b_H$ reduction and cyt *c* re-reduction. Sections A and B correspond to the data obtained using the wild-type strain pMTS1 and the mutants G146A and V, respectively. In each case, left panel shows the cyt $b_H$ reduction kinetics observed in the presence of 10 $\mu$M antimycin, and after addition of 5 $\mu$M myxothiazol, and right panel the cyt *c* re-reduction kinetics in the absence of any inhibitor, in the presence of 10 $\mu$M antimycin and after addition of 5 $\mu$M myxothiazol. In all cases the measurements were performed as described in Section 2. The traces shown were generated by averaging the data obtained for a minimum of 20 single flashes of light, and the system was allowed to re-equilibrate for several minutes between each flash.

## 3. Results

### 3.1. Phenotypic properties of cyt b G146A and V mutants

The cyt *b* mutants G146A and V were unable to grow by photosynthesis, indicating that they contained defective $bc_1$ complexes. Unexpectedly, G146V substitution also affected partially respiratory growth since it yielded a mixture of smaller (5 $\mu$m in diameter) and larger (12 $\mu$m in diameter) size colonies on MPYE plates after 48–72 h incubation, and reverted more readily to $Ps^+$ phenotype. Under similar growth conditions, strains containing a wild-type $bc_1$ complex or a complete deletion of it yielded colonies of 15 $\mu$m or 10 $\mu$m diameter, respectively. Considering that this growth defect was not observed in the absence of the $bc_1$ complex, it is unrelated to the function of this complex, and therefore was not pursued further. Next, SDS-PAGE and Western blot analyses of chromatophore membranes with subunit-specific antibodies indicated that both G146A and V mutants contained the three subunits of the $bc_1$ complex at a wild-type level. Finally, optical difference spectra confirmed that the total amounts of the *b* and *c* cytochromes in these mutants were similar to those of a wild-type strain (data not shown). Thus, the *R. capsulatus* mutants G146A and V, unlike their yeast homologue G131S, were able to produce properly assembled but inactive $bc_1$ complexes, lending themselves to further detailed analysis.

### 3.2. Biochemical and biophysical analyses of cyt b G146A and V mutants

First, the steady-state level of the DBH dependent cyt *c* reductase activity was determined in both G146A and V mutants, and found to be about 10% of that detected in the parental strain pMTS1/MT-RBC1, an amount which was consistent with their $Ps^-$ phenotype (Table 1). Next, flash-induced single turnover kinetics were monitored in these mutants, and these measurements indicated that electron transfer rates were significantly reduced in both cases. The rate of electron transfer from $Q_o$ site to $b_H$ was decreased by approx. 36-fold at 100 mV, whereas that of cyt *c* re-reduction was slowed down by approx. 20-fold (Fig. 2B, and Table 1) when compared with those of a wild-type strain (Fig. 2A and Table 1). Thus, the data clearly indicated that the $Q_o$ site of the mutant $bc_1$ complexes were unable to perform $QH_2$ oxidation. To determine whether the

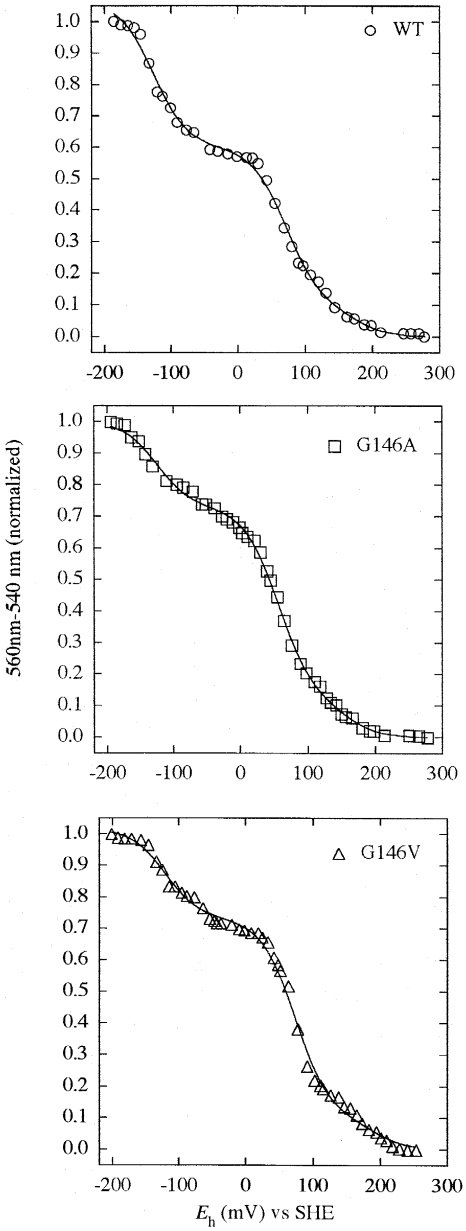


Fig. 3. Optical potentiometric redox titrations of chromatophores derived from the wild type *R. capsulatus* strain pMTS1 (WT, upper panel) and the cyt *b* mutants G146A (middle panel) and G146V (lower panel). The dark equilibrium titrations were performed as described in Section 2, and the data points obtained were fitted to a Nernst equation ($n=1$) to calculate the redox mid-point potentials ($E_{m,7}$) of the hemes $b_H$ and $b_L$.

Table 2
Redox midpoint potentials ($E_{m,7}$) and $g_z$ values of the EPR signals of the hemes $b_L$ and $b_H$ in *R. capsulatus* G146A and V mutants

| Strains | Redox titrations | | EPR Spectra | |
|---|---|---|---|---|
| | $E_{m,7}$ ($b_L$) (mV) | $E_{m,7}$ ($b_H$) (mV) | $g_z$ ($b_L$) | $g_z$ ($b_H$) |
| pMTS1 (wt) | −126 | 71 | 3.791 | 3.463 |
| pBG146A | −126 | 56 | 3.713 | 3.497 |
| pBG146V | −120 | 73 | 3.722 | 3.473 |

lack of $Q_o$ site catalysis was due to perturbed redox midpoint potentials of the hemes $b_L$ and $b_H$, these redox groups were titrated potentiometrically in the dark. In the case of G146A, the $E_{m,7}$ for heme $b_H$ was found to be slightly lower (56 mV) than that of a wild-type $bc_1$ complex (71 mV) or that of G146V mutant (72 mV) (Fig. 3, Table 2). However, this difference was not considered significant enough to account for the lack of efficient $QH_2$ oxidation in the mutants. Note that these titration curves can also be fit to three cyt *b* components including cyt $b_{150}$. However, since cyt $b_{150}$ does not seem to change drastically in these strains, only two components were used for fitting the data shown in Fig. 3.

Next, the $Q_o$ site occupancy was monitored by EPR spectroscopy using the known interaction between the [2Fe-2S] cluster of the FeS protein and $Q/QH_2$ residing at the $Q_o$ site. Previous work has established that in a wild-type strain (i.e., $Q_o$ site is fully occupied) a characteristic EPR signal with a $g_x$ value of 1.800 was observed where the $Q_{pool}$ is fully oxidized at an $E_h$ around 200 mV, and that this signal shifts to a $g_x$ value of 1.777 when the $E_h$ is decreased to around 0 mV, when the $Q_{pool}$ is fully reduced [10,12]. On the other hand, if the binding of $Q/QH_2$ to $Q_o$ site is modified either by extraction of the $Q_{pool}$, or by mutations affecting this site, then the $g_x$ signal shifts to values lower than the latter, ultimately reaching a $g_x$ value of 1.765 when the site is completely empty [10]. The EPR spectra presented in Fig. 4 indicate that G146A has a $g_x$ value of 1.776 at an $E_h$ of 197 mV, thus a nearly empty $Q_o$ site (Fig. 4B, lower left trace). Clearly, the $g_x$ signal observed in Fig. 4 exhibits some heterogeneity which reflects the presence of more than one population of $Q_o$ site of modified occupancy (see Ding et al. [10]).

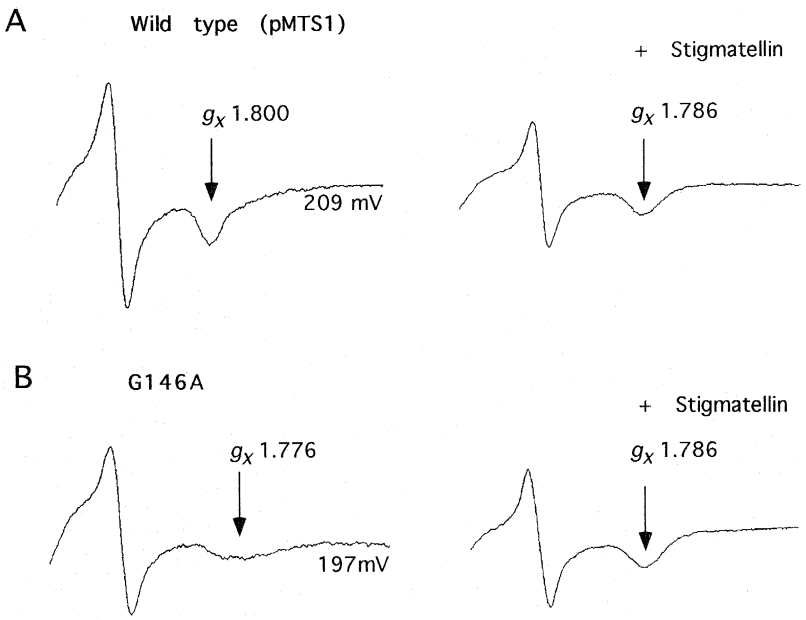


Fig. 4. EPR spectra of the [2Fe-2S] cluster of the $bc_1$ complex in the absence (left panel), and presence (right panel) of the $Q_o$ site inhibitor stigmatellin. Note that a two-fold smaller scale was used for the spectra shown on the left panel. A, spectrum obtained using chromatophores of pMTS1 producing a wild-type $bc_1$ complex ($E_h$ = 209 mV), and B, that of the cyt *b* mutant G146A ($E_h$ = 197 mV).

Nonetheless, note that this site can still bind the $Q_o$ site inhibitor stigmatellin efficiently, and yield a characteristic signal with a $g_x$ value of 1.786, identical to that observed with a wild-type $bc_1$ complex (Fig. 4A, upper right trace). Similar data were also obtained with G146V and not presented. Further, titration in the presence or absence of stigmatellin of the $g_y$ signal of the [2Fe-2S] cluster indicated that neither the midpoint potential of this latter redox center ($E_{m,7}$ of 308 mV and 288 mV for wild-type and G146A, respectively) nor its response to this inhibitor was modified drastically in the G146 mutants (Fig. 5). The overall data therefore clearly indicated that substitution of position 146 with an amino acid of a side chain slightly larger than a proton such as a methyl group (i.e., G to A substitution) yields an inactive $bc_1$ complex by perturbing $Q/QH_2$ occupancy of the $Q_o$ site. However, whether these mutations empty the $Q_o$ site by simply hindering the accessibility or the binding of $Q/QH_2$ to the site, or by other means is unknown.

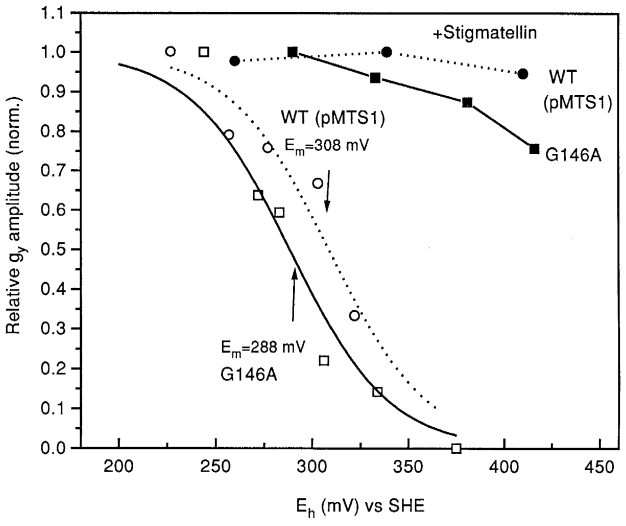


Fig. 5. EPR redox titrations of [2Fe-2S] clusters of wild-type and G146A mutant of *R. capsulatus*. An amount of chromatophores containing 600 $\mu$M BChl was resuspended in 50 mM MOPS (pH 7.0) and 100 mM KCl in the presence of 25 mM TMPD, DAD and 1,2 NQ 4S. The $E_h$ of the suspension was poised above 400 mV using potassium ferricyanide, and 250 $\mu$l aliquots were withdrawn at desired $E_h$ values obtained by adding sodium ascorbate. When an $E_h$ of 200 mV was reached, a final concentration of 40 $\mu$M stigmatellin, and enough potassium ferricyanide was added to the remaining suspension, and the titration was continued as above. EPR spectra were measured as described in Section 2, the amplitude of the $g_y$ signal was normalized and fit to a Nernst equation for $n=1$ to deduce the $E_m$ values shown.

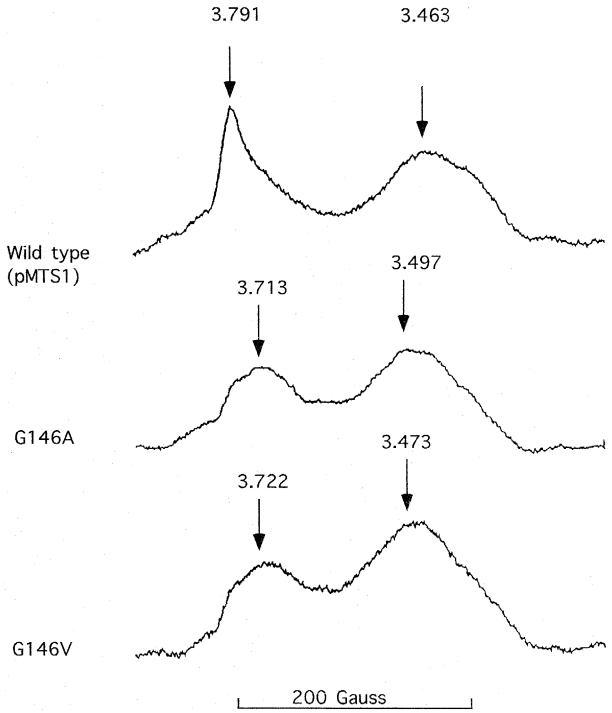


Fig. 6. EPR Spectra of the hemes $b_L$ and $b_H$ from wild-type (pMTS1, upper trace) *R. capsulatus* $bc_1$ complex and the cyt *b* mutants G146A (middle trace) and G146V (lower trace). Chromatophores used in this experiment were prepared at high concentration [Bchl = 1.2 mM], and were reduced with ascorbate [20 mM final concentration] prior to recording the spectra.

Lastly, EPR spectra of the hemes $b_L$ and $b_H$ were recorded to see whether any experimental data could be obtained to support the initial proposal of Tron et al. [14], that position 146 should be occupied by an amino acid with a small side chain for proper packing of cyt *b* heme $b_L$. We reasoned that if a larger side chain occupies position 146 and perturbs the spatial conformation of heme $b_L$, then the EPR line shape of this heme group could be modified since the resonance positions and characteristic line shapes of the hemes $b_H$ and $b_L$ are related to specific spatial interactions between the heme-iron and the imidazole rings of the liganding histidines [22–24]. Using highly concentrated membrane samples under the conditions described in Section 2, EPR spectra of the hemes $b_H$ and $b_L$ were recorded in both G146A and V mutants (Fig. 6). These data revealed that in both G146A and V mutants, the EPR line shape attributed to the heme

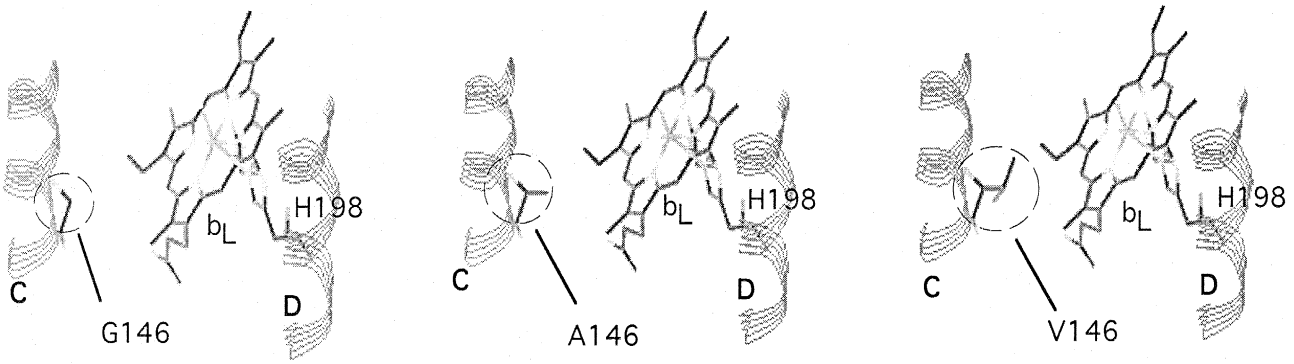


Fig. 7. A hypothetical model to illustrate the possible local interactions between the amino acid side chains at position 146 of cyt *b* and the chemical groups of the porphyrin ring of heme $b_L$ in the wild-type and the G146A and G146V mutant $bc_1$ complexes.

$b_L$ of cyt *b* was modified drastically, and the corresponding $g_z$ values were shifted from 3.791 in a wild-type strain to 3.713 and 3.722 in G146A and V, respectively. On the other hand, in both G146A and V the EPR line shapes and the $g_z$ value corresponding to heme $b_H$ were around 3.463 ($g_z$ 3.497 and 3.473 for G146A and V, respectively) and similar to those observed with a wild-type $bc_1$ complex (Fig. 6). Thus, the size of the amino acid side chain at position 146 influences mainly the EPR characteristics, hence the spatial conformation, of heme $b_L$.

It could be thought that a conformational change of heme $b_L$ may also affect the rate of electron transfer from $b_L$ to $b_H$, which would then lead to slow cyt *b* reduction rates observed in the presence of antimycin in Fig. 2. This possibility was tested by measuring the non-physiological, antimycin-sensitive reverse electron transfer rates at pH 9.0 in the presence of myxothiazol [13]. The results obtained indicated that no significant difference was observed for $Q_i$ to cyt $b_H$ electron transfer rates between the wild-type and the G146A mutant (300 $s^{-1}$ and 242 $s^{-1}$ respectively) (data not shown).

## 4. Discussion

Position G146 of *R. capsulatus* cyt *b* is one of the four universally conserved G residues of this protein (the three others being G48, G62 and G132) proposed to be involved in the proper packing of the porphrin ring of the hemes $b_H$ and $b_L$. In this work, the role of G146 was investigated using site-directed mutagenesis in combination with biochemical and biophysical characterizations of the mutants obtained. The data clearly indicate that G146 is very important for heme $b_L$ packing and $Q_o$ site structure, hence for a functional $bc_1$ complex. Its substitution with a residue of a slightly larger size than G, such as an A, inactivates the $bc_1$ complex drastically by perturbing the spatial conformation of heme $b_L$ and the $Q_o$ site occupancy, leading to slower electron transfer kinetics (Fig. 7). Previous studies on the coordination environment of mitochondrial cytochromes *b* [25] and on the EPR line shapes and characteristics of these heme groups have attributed their characteristic high $g_z$ values to 'strained' or sterically hindered bis-imidazole coordination [26]. Apparently to maintain a correct angle between the heme Fe and the nitrogen atom of the imidazole group of the axial histidine ligand the porphyrin ring of heme needs to extend through a space surrounding G146 (Fig. 7). Thus, it is conceivable that an increase in the volume of the amino acid side chain at this position constrains the available space in this region of the $bc_1$ complex to tilt the porphyrin ring and also to perturb the $Q/QH_2$ occupancy or binding of the $Q_o$ site. Both of these effects were readily evidenced by changes accompanying the EPR characteristics of the $Q_o$ site and the heme $b_L$ (Fig. 7). Note that this is the first experimental evidence supporting the proposal of Tron et al. [14], and demonstrating that polypeptide packing at this region of cyt *b* is critical for an active $Q_o$ site. Possibly, a similar conclusion could

also be expected in respect to the roles of the three other G residues mentioned above and their effects on appropriate hemes and Q sites of cyt *b*.

In the absence of the three-dimensional structure of the $bc_1$ complex with an atomic resolution [27], it remains difficult to define rigorously whether the perturbations described here render the $bc_1$ complex inactive by modifying solely the properties of heme $b_L$ or the occupancy of the $Q_o$ site, or by a combination of both these effects. Undoubtedly, a more precise definition of the role of these residues, and the effects of the amino acids substituting them, will await the resolution of the three dimensional structure of the $bc_1$ complex which, fortunately, is now imminent [27].

## Acknowledgements

This work was supported by NIH Grant GM 38237 to F.D. and 27309 to P.L.D. The authors thank B. Wong for her help during the construction of the mutants, and Drs. Dan Robertson, Brian Gibney, Eryl Sharp and Tomoko Ohnishi for helpful discussion and critical reading of the manuscript, and Brian Gibney for help with the EPR spectroscopy.

## References

[1] Gennis, R.B., Barquera, B., Hacker, B., Van Doren, S.R., Arnaud, S., Crofts, A.R., Davidson, E., Gray, K.A. and Daldal, F. (1993) J. Bioenerg. Biomembr. 25, 195–209.
[2] Trumpower, B. and Gennis, R.B. (1994) Annu. Rev. Biochem. 63, 675–716.
[3] Brandt, U. and Trumpower, B. (1994) Crit. Rev. Biochem. Mol. Biol. 29, 165–197.
[4] Gray, K.A. and Daldal, F. (1995) in Anoxygenic Photosynthetic Bacteria (Blankenship, R.E., Madigan, M.T. and Bauer, C., Eds.), pp. 747–774. Kluwer Academic Publications. Dordrecht, The Netherlands.
[5] Yun, C.H., Crofts, A.R. and Gennis, R.B. (1991) Biochemistry 30, 6747–6754.
[6] Robertson, D.E. and Dutton, P.L. (1988) Biochim. Biophys. Acta 935, 273–291.
[7] Robertson, D.E., Daldal, F. and Dutton, P.L. (1990) Biochemistry 29, 11249–11260.
[8] Atta-Asafo-Adjei, E. and Daldal, F. (1991) Proc. Natl. Acad. Sci. USA 88, 492–496.
[9] Tokito, M.K. and Daldal, F. (1993) Mol. Microbiol. 9, 965–978.
[10] Ding, H., Robertson, D.E., Daldal, F. and Dutton, P.L. (1992) Biochemistry 31, 3144– 3158.
[11] Ding, H., Moser, C.C., Robertson, D.E., Tokito, M.K., Daldal, F. and Dutton, P.L. (1995) Biochemistry 34, 15979–15996.
[12] Ding, H., Daldal, F. and Dutton, P.L. (1995) Biochemistry 34, 15997–16003.
[13] Saribaş, A.S., Ding, H., Dutton, P.L. and Daldal, F. (1995) Biochemistry 34, 16004– 16012.
[14] Tron, T., Crimi, M., Colson, A.-M., Degli Esposti, M. (1991) Eur. J. Biochem. 199, 753–760.
[15] Yun, C.H., Wang, Z., Crofts, A.R. and Gennis, R.B. (1992) J. Biol. Chem. 267, 5901– 5909.
[16] Lemesle-Meunier, D., Brivet-Chevillotte, P., diRago, J.P., Slonimski, P.P., Bruel, C., Tron, T. and Forget, N. (1993) J. Biol. Chem. 268, 15626–15632.
[17] Daldal, F., Tokito, M.K., Davidson, E. and Faham, M. (1989) EMBO J. 8, 3951–3961.
[18] Davidson, E., Ohnishi, T., Atta-Asafo-Adjei, E. and Daldal, F. (1992) Biochemistry 31, 3342–3351.
[19] Lowry, O.H., Rosebrough, N.J., Farr, A.L. and Randal, R.J. (1951) J. Biol. Chem. 193, 1571–1579.
[20] Dutton, P.L. (1978) Methods Enzymol. 5, 411–435.
[21] Gray, K.A., Dutton, P.L. and Daldal, F. (1994) Biochemistry 33, 723–733.
[22] Robertson, D.E., Ding, H., Chelminski, P.R., Slaughter, C., Hsu, J., Moonraw, C., Tokito, M., Daldal, F. and Dutton, P.L. (1993) Biochemistry 32, 1310–1317.
[23] Salerno, J.C., Osgood, M.P., Kim, C.H. and King, T.E. (1989) J. Biol. Chem. 264, 15398–15403.
[24] McCurley, J.P., Miki, T., Yu, L. and Yu, C.-A. (1990) Biochim. Biophys. Acta 1020, 176–186.
[25] Carter, K.R., Tsai, A. and Palmer, G. (1981) FEBS Lett. 132, 243–246.
[26] Salerno, J.C. (1984) J. Biol. Chem. 259, 2331–2336.
[27] Xia, D., Yu, C.-A., Deisenhofer, J., Xia, J.-Z. and Yu, L. (1996) Biophys. J. 70, A253
[28] Degli-Esposti, M., De Vries, S., Crimi, M., Gelli, A., Patarnello, T. and Meyer, A. (1993) Biochim. Biophys. Acta 1143, 243–271.
[29] Berden, J.A. and Slater, E.C. (1970) Biochim. Biophys. Acta 216, 237–249.